Science of the Total Environment 783 (2021) 146973

Contents lists available at ScienceDirect

Science of the Total Environment

journal homepage: www.elsevier.com/locate/scitotenv

Global assessment of future sectoral water scarcity under adaptive inner-basin water allocation measures

Zhongwei Huang [a,b], Xingcai Liu [b], Siao Sun [b], Yin Tang [b], Xing Yuan [a], Qiuhong Tang [b,c,*]

[a] School of Hydrology and Water Resources, Nanjing University of Information Science and Technology, Nanjing, China
[b] Key Laboratory of Water Cycle and Related Land Surface Processes, Institute of Geographic Sciences and Natural Resources Research, Chinese Academy of Sciences, Beijing, China
[c] University of Chinese Academy of Sciences, Beijing, China

HIGHLIGHTS

- Adaptive measures were considered in future global water scarcity assessment.
- The impact of adaptive measures on water scarcity was analyzed.
- Global water scarcity would intensify, especially in arid and semi-arid areas.
- Adaptive measures could mitigate water scarcity for nonagricultural sectors.
- Adaptive measures might aggravate agricultural water scarcity.

GRAPHICAL ABSTRACT

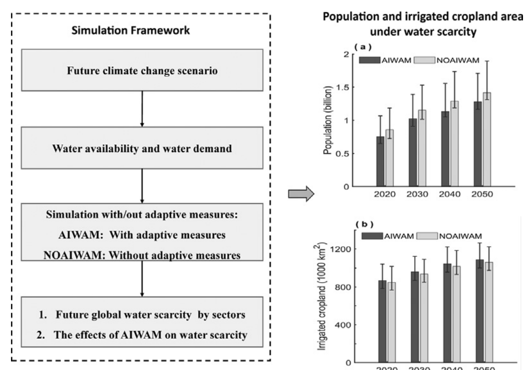

ARTICLE INFO

Article history:
Received 19 December 2020
Received in revised form 31 March 2021
Accepted 1 April 2021
Available online 7 April 2021

Editor: Ashantha Goonetilleke

Keywords:
Water scarcity
Water deficit
Adaptive measures
Water allocation
Water demand

ABSTRACT

Water scarcity has become a major threat to sustainable development under climate change. To reduce the population exposure to water scarcity and improve universal access to safe drinking water are important targets of the Sustainable Development Goal (SDG) 6 in the near future. This study aims to examine the potential of applying adaptive inner-basin water allocation measures (AIWAM), which were not explicitly considered in previous studies, for mitigating water scarcity in the future period (2020–2050). By incorporating AIWAM in water scarcity assessment, nonagricultural water uses are assumed to have high priority over agricultural water use and thus would receive more water supply. Results show that global water deficit is projected to be ~3241.9 km^3/yr in 2050, and severe water scarcity is mainly found in arid and semi-arid regions, e.g. Western US, Northern China, and the Middle East. Future warming climate and socioeconomic development tend to aggravate global water scarcity, particularly in Northern Africa, Central Asia, and the Middle East. The application of AIWAM could significantly mitigate water scarcity for nonagricultural sectors by leading to a decrease of global population subject to water scarcity by 12% in 2050 when compared to that without AIWAM. However, this is at the cost of reducing water availability for agricultural sector in the upstream areas, resulting in an increase of global irrigated cropland exposed to water scarcity by 6%. Nevertheless, AIWAM provides a useful scenario that helps design strategies for reducing future population exposure to water scarcity, particularly in densely populated basins and regions. Our findings highlight increasing water use competition across sectors between upstream and downstream areas, and the results provide useful information to develop adaptation strategies towards sustainable water management.

* Corresponding author at: Key Laboratory of Water Cycle and Related Land Surface Processes, Institute of Geographic Sciences and Natural Resources Research, Chinese Academy of Sciences, Beijing 100101, China.
E-mail address: tangqh@igsnrr.ac.cn (Q. Tang).

https://doi.org/10.1016/j.scitotenv.2021.146973
0048-9697/

1. Introduction

As a result of increasing in human water demand driven by the rapid global population growth, economic development and rising living standard, water scarcity has become one major threat to the sustainable development of human society. Water scarcity may result in multiple social and environmental issues, such as drinking water shortage (Oki and Kanae, 2006; Vörösmarty et al., 2010), reduction of crop production (Rockström et al., 2009; Gerten et al., 2011), and water quality degradation (Cheng et al., 2009; Liu et al., 2016). Furthermore, global water scarcity will change along with future climate change and socioeconomic development (Hejazi et al., 2014; Greve et al., 2018). Therefore, it is essential to understand global water scarcity conditions under future changing environment, which is a prerequisite for developing planning and management policies to mitigate water scarcity at the global, regional, and local scales.

Current water scarcity projections are mostly based on water availability and water demand simulations from global hydrological models (GHMs), taking into account the impacts of both future climate change and socioeconomic development (Hanasaki et al., 2013a, 2013b; Hejazi et al., 2015). Furthermore, a wealth of studies have addressed the role of multiple adaptive options in coping with water scarcity conditions, e.g. irrigation efficiency improvement (Flörke et al., 2018), inter-basin water transfer infrastructures (Barnett et al., 2015; Yin et al., 2020), sea water desalination (Hanasaki et al., 2016), and virtual water trade (Zhao et al., 2015; Pastor et al., 2019). Previous water scarcity assessments often compared water demand with water availability to assess water scarcity at the local, regional, and global scales. Water demand was estimated as the sum of water demands from agricultural, domestic and industrial sectors in most studies (Wada et al., 2016; Huang et al., 2018; Joseph et al., 2020), whereas water availability was calculated in different ways, such as from runoff (e.g. Hejazi et al., 2014), natural river discharge (e.g. Vörösmarty et al., 2005), and the difference between natural river discharge and environmental flow (e.g. Hanasaki et al., 2013b). The allocation of available water resources between upstream and downstream regions is important for water scarcity assessments (Yan et al., 2018; Gaaloul et al., 2020). Different treatments of water abstraction in upstream areas may affect water scarcity assessment to a significant extent. As downstream areas usually rely on water supply from upstream, ignoring the impacts of upstream water abstraction on downstream water availability would underestimate water scarcity in the downstream areas. To overcome this issue, Munia et al. (2016) conducted the first assessment of water scarcity by considering upstream water use as the first priority, and analyzed the effects of upstream water abstraction on downstream water scarcity. Going beyond this, Liu et al. (2019) further compared the differences of water scarcity assessment by using different water scarcity indices which were calculated as the ratios of water demand to locally generated runoff, to natural streamflow, and to natural streamflow minus upstream water abstraction.

However, as important adaptive measures to cope with water scarcity, the inner-basin water allocation measures, which were often designed to redistribute available water resources within a basin in practice, has not been incorporated in most large-scale water scarcity assessments. For example, the Yellow River Conservancy Commission (YRCC) in China implemented a flow regulation rule that sets an upper limit on upstream water abstraction in order to mitigate downstream water scarcity in the Yellow River basin (Cai and Rosegrant, 2004; YRCC, 2013; Yin et al., 2017). Similar inner-basin water allocation measures have been applied in the Indus River basin (Zawahri, 2009), the Euphrates and Tigris River basins (Kliot, 2005), and the Middle East and Northern Africa (Brown, 2000). The inner-basin water allocation measures aim to cope with water scarcity due to inter-sectoral water competition between upstream and downstream areas. The concept of inner-basin water allocation measures is within the realm of integrated water resources management (IWRM), which is designed to achieve sustainable use of water resources (Biswas, 2004), and has been widely used in regional water management and planning (Pires et al., 2017; Wang et al., 2019; Chang et al., 2020). However, because inner-basin water allocation measures were often applied at basin and local scales according to the local governmental development goals, previous water scarcity assessment, especially large-scale assessment, often set upstream often have the highest priority to use the available water resources. Neglecting the inner-basin water allocation measures may result in significant biases in water availability and water scarcity estimates. Furthermore, the intensity and frequency of precipitation will also change under future global warming, leading to significant changes in local runoff (Tang and Oki, 2016; Yin et al., 2021), which will affect spatial and temporal distributions of available water resources (Tang and Lettenmaier, 2012; Zhou et al., 2017; Tang, 2020). Human water demand is also expected to increase along with socioeconomic development and population growth (Wada et al., 2016). Thus, regional water scarcity would show a changing pattern. The adaptive inner-basin water allocation measures (AIWAM), which largely reflect the ability of humans to reduce population exposure to water scarcity to partly achieve the sustainable development goal (SDG) 6 (i.e. clean water and sanitation), also evolve with a changing human adaptation capacity under a changing environment. The water scarcity assessment with AIWAM would provide an adaptation scenario that depicts the change in water scarcity with reallocated water resources under future climate change.

This study utilized the hydrological simulations from multiple GHMs and performed an assessment of future global water scarcity at the grid cell level ($0.5° \times 0.5°$) during 2020–2050 by incorporating AIWAM. The objectives of this study include: 1) to assess the spatiotemporal patterns of future global water scarcity during 2020–2050 under climate change and socioeconomic development, and 2) to analyze the effects of AIWAM on global sectoral water scarcity. The remainder of this paper was organized as follows: the data and methodologies were represented in "data and methods" section; findings about future global sectoral water scarcity under AIWAM were represented in the "results" section; a comparison of estimation in this study with previous results, limitations of the methodologies and broader implications of the results were discussed in the "discussion" section; lastly, conclusions were drawn.

2. Data and methods

In this study, to assess global water scarcity under future climate change and socioeconomic development, the annual natural runoff and sectoral water demand datasets from GHMs were firstly obtained (details in Sections 2.2 and 2.3). Then, AIWAM were incorporated into the assessment of future global sectoral water scarcity (Sections 2.4 and 2.5). To assess the effects of AIWAM on sectoral water scarcity, another simulation was designed, which set upstream water abstraction as the first priority over downstream water demand, in contrast to the simulation with AIWAM (details in Section 2.6). A schematic representation of water scarcity assessment in this study was shown in Fig. 1. The details of assessment of future global water scarcity were represented in subsections below.

2.1. Climate change scenario

The representative concentration pathways (RCP) and shared socioeconomic pathway (SSP) framework consider the effects of both climate change and socioeconomic development in a changing environment, and has been widely used in future water scarcity projections (Hanasaki et al., 2013b; Greve et al., 2018). This study adopted the middle of road scenario RCP6.0-SSP2 combination (Fricko et al., 2017). SSP2 depicts the evolution of future socioeconomic development as the socioeconomic trends of recent decades continue. The projected global population under the middle of road scenario (i.e. SSP2) grows to

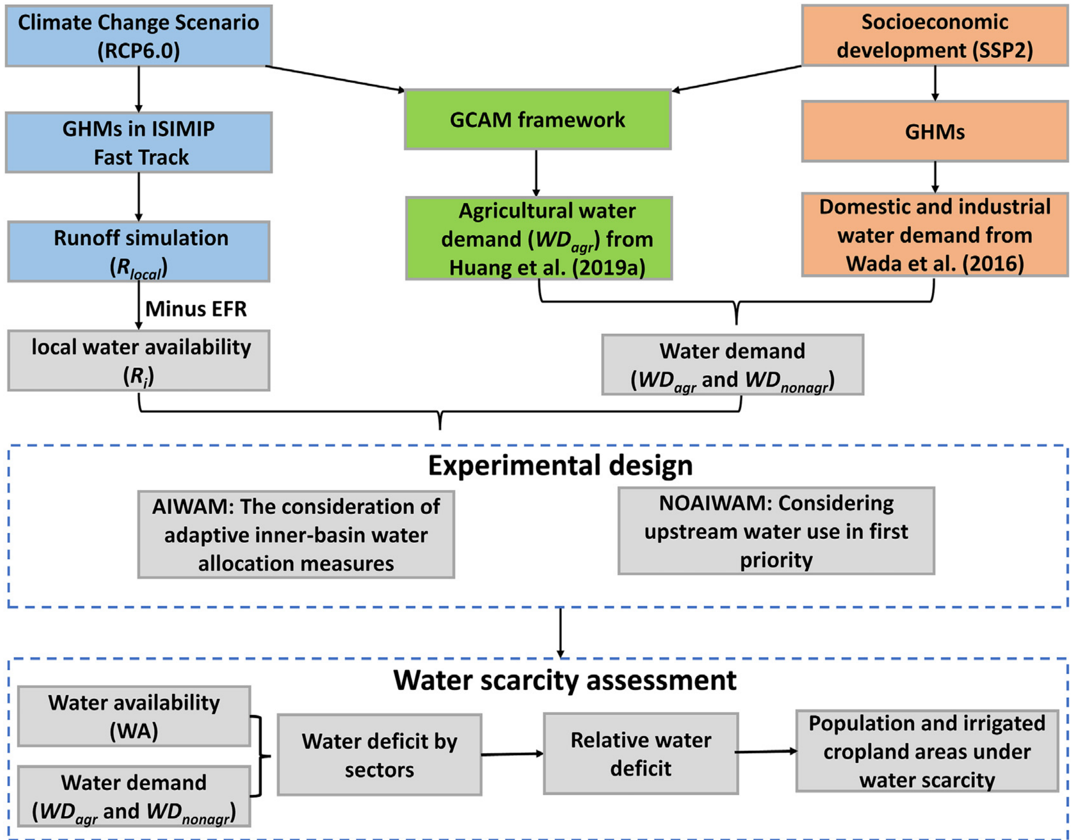

Fig. 1. A schematic representation of future global water scarcity assessment under AIWAM. The blue boxes were for the description of water availability (in Section 2.2); while green and orange boxes represented processes of agricultural and nonagricultural water demand (Section 2.3), respectively. After getting local water availability and water demand, two simulations were designed, and sectoral water scarcity conditions were estimated based on different calculation rules under two simulations. A detailed example of water scarcity calculation was shown in Supplementary Fig. S1.

around 9.2 billion in the 2050s, peaks around 9.4 billion in the 2070s, and then declines to about 9.0 billion by the end of this century (Samir and Wolfgang, 2017). RCP6.0 is a stabilization without overshoot scenario in which the total radiative forcing level reaches 6 W/m^2 at stabilization after 2100, which indicates a global warming of about 4 °C by 2100 (van Vuuren et al., 2014).

There are many studies using different RCPs to consider future projections of water availability (Hanasaki et al., 2013b; Hejazi et al., 2014; Yin et al., 2017; Ferguson et al., 2018). The global pattern of water availability change using different RCPs is generally consistent (Zhang et al., 2018). Water demand was also projected under different socioeconomic development scenarios in previous studies (Hanasaki et al., 2013a; Wada et al., 2016). A single scenario would lead to a narrow representation of future water scarcity, whereas the inclusion of multiple SSP-RCP scenarios could provide more insights into future water scarcity associated with various climate change and socioeconomic development scenarios (O'Neill et al., 2014; Greve et al., 2018). Since the main purpose of this study was to investigate the effects of AIWAM on future sectoral water scarcity, only one combined RCP-SSP scenario (i.e. RCP6.0-SSP2 scenario) was adopted for simplicity. The RCP6.0-SSP2 scenario represents moderate evolution of future global water scarcity, which might exclude extreme scenarios that would be less likely to happen with the ongoing efforts devoted to climate change mitigation and adaptation (van Vuuren et al., 2014; Fricko et al., 2017).

2.2. Water availability

The annual total runoff was obtained from the Inter-Sectoral Impact Model Inter-comparison Project Phase Fast-track (ISI-MIP, https://www.isimip.org/). This runoff dataset was derived for the period 2005–2065 at a global 0.5° × 0.5° spatial resolution from an ensemble of five GHMs, i.e. H08 (Hanasaki et al., 2008a, 2008b), VIC (Liang et al., 1994), MPI-HM (Stacke and Hagemann, 2012), PCR-GLOBWB (van Beek et al., 2011; Wada et al., 2011), and WBMplus (Wisser et al., 2010). These GHMs were forced by climate projections from 5 general circulation models (GCMs) in the fifth phase of the Coupled Model Intercomparison Project (CMIP5, Hempel et al., 2013; Warszawski et al., 2014), namely HadGEM2-ES, NorES1-M, IPSL-CM5A-LR, MIROC-ESM-CHEM and GFDL-ESM2M under the RCP6.0 scenario (details in Supplementary Table S1). These climate datasets from GCMs were bias-corrected using the WATCH climate data for the overlapping period using a statistical bias correction method which was based on transfer functions generated to map the distribution of the simulated historical data to that of the observations, and the climate projections reserved the long-term trends in temperature and precipitation projections (Piani et al., 2010; Hempel et al., 2013). Parameterizations of hydrological processes were different among GHMs. H08 considered the energy balance explicitly and used the bulk formula in the evapotranspiration scheme. VIC estimated snow by energy balance and used Penman Monteith formula in evapotranspiration module. MPI-HM, PCR-GLOBWB and WBMplus did not include the energy balance, but used the Penman Monteith or Hammon formulas in their evapotranspiration schemes, and a degree-day calculation method or temperature and precipitation based empirical formula in snow scheme. In terms of the runoff generation, all GHMs used a saturation excess formula, although the formula varied across GHMs. A detail representation of these GHMs was referred to Supplementary Table S2 and related literature of these models.

Annual total runoff from the GHMs, which has been widely used as an indicator of renewable water resources in many regional and global water scarcity assessment (Schewe et al., 2014; Yin et al., 2017; Liu et al., 2019), was considered as the annual water availability in this study. The total runoff consists of the locally generated surface runoff and baseflow, as well as the incoming runoff from upstream grid cells following the river routing map. This study didn't consider water depletion from lakes, aquifers and sub-surface reservoirs, and assumed a long-term equilibrium in the storages of these aquifers, because their water depletion values were unknown and difficult to measure.

Environmental flow requirement (EFR) was taken into consideration in this study. Unlike previous studies in which EFR was calculated by maintaining a minimum flow, this study predefined a reservation of fresh water resources for environmental purposes. However, the relationships between ecological consequences and flow regimes varied over regions and river ecosystems in large scale assessment. Pastor et al. (2014) estimated that 25–46% (with 37% in 11 selected rivers) of annual discharge was required to sustain EFR and that the ratio of EFR to annual flow did not show strong differences across regions in the world. This study adopted global EFR estimation from Pastor et al. (2014) and assumed that 40% of annual local runoff was appropriated to maintain ecological integrity, which was consistent with previous studies, e.g. Liu et al. (2019). Therefore, 60% of the locally generated runoff was calculated for local water availability:

$$R_i = R_{local} - EFR = 0.6 * R_{local}, \tag{1}$$

where R_i was water availability in grid i and R_{local} was locally generated runoff from multiple GHMs (m^3). Local water availability was assessed at an annual basis for each year during 2005–2065, and the 31-year moving average value was used to reduce the impact of inter-annual variability.

2.3. Water demand

Agricultural water demand (WD_{agr}) was estimated by the Global Change Assessment Model (GCAM) and two of its ancillary modeling tools, namely Demeter and Xanthos, which can well represent the effects of future climate and land use changes, especially future changes in cropland area driven by population growth and socioeconomic development (Edmonds et al., 1997; Huang et al., 2019a; Kim et al., 2006; Vernon et al., 2018) WD_{agr} was calculated by multiplying the crop water requirement per unit of irrigated area by the area of irrigated cropland and irrigation efficiency. In this study, climate forcing from 5 GCMs was also served as climate inputs for hydrological model (i.e. Xanthos in GCAM framework), the same as that for GHMs (see Section 2.2), and crop specific water requirement per unit of irrigated cropland were calculated (Huang et al., 2019a). Future land use (especially irrigated cropland) was projected by GCAM at the regional level under SSP2 scenario (Calvin et al., 2014, 2018; Chen et al., 2020). Then, Demeter was applied to disaggregate the cropland area from the regional to grid scale (West et al., 2014; Le Page et al., 2016; Vernon et al., 2018). Irrigation efficiency across global major regions under SSP2 scenario was obtained from Chaturvedi et al. (2015). In general, global WD_{agr} was generated at a spatial resolution of 0.5° × 0.5° at the monthly time scale, the monthly WD_{agr} was then aggregated to annual scale. The 31-yr moving average value of WD_{agr} at the grid level was used to exclude the impact of inter-annual variability on the changing signal.

Domestic and industrial water demands during 2020–2050, which were obtained from the Water Futures and Solutions (WFaS) project (Wada et al., 2016), were the ensemble mean of the water demand simulations by 3 GHMs, namely H08 (Hanasaki et al., 2013a, 2013b), PCR-GLOBWB (Wada et al., 2014) and WaterGAP (Flörke et al., 2013). In these models, domestic and industrial water demand was calculated by time-series regression over individual regions and countries driven by future socio-economic factors, e.g. population, Gross Domestic Product (GDP) per capita and technological changes. National or regional domestic and industrial water demand was disaggregated to 0.5° × 0.5° grid cell scale based on gridded population density map or other socioeconomic factors (e.g. electricity generation) (Hanasaki et al., 2013a; Wada et al., 2014; Flörke et al., 2013).

2.4. Adaptive inner-basin water allocation measures (AIWAM)

AIWAM were incorporated into future global water scarcity assessment, which reallocated available water resources within a basin. In fact, the water allocation mechanism was complex and various allocation mechanisms were used in practice according to development goals across countries and regions. The SDG6 (clean water and sanitation) targets to mitigate water scarcity, improve access to safe drinking water and sanitation services in view of the fact that about 30% of global population lack access to safely managed drinking water services (UN, 2018). To partly address one of the targets of the SDG 6 and achieve optimal benefit at the global scale, this study assumed that nonagricultural (domestic and industrial) water uses would have higher priority over agricultural water use in AIWAM, which aimed to reduce population exposed to water scarcity. It is to some extent reasonable that limited water resources are firstly appropriate to improve human life and maintain necessary industry which may have more added-value than agricultural products (Hanasaki et al., 2018). Thus, in the AIWAM, available water resources are appropriated to grid cells based on the spatial variation of population density in the future, assuming that the grid cells with high population would have high water resources quota within a basin.

As AIWAM changed the spatial distribution of available water resources from natural water availability, water availability quota at grid scale in a basin was calculated by the following steps. Firstly, the total water availability in a basin (Q) was calculated as the sum of water availability in all the grid cells:

$$Q = \sum_{i=1}^{n} R_i, \tag{2}$$

where R_i was water availability calculated by local generated annual total runoff minus local EFR (shown in Eq. (1)), and n was the total number of grid cells in the basin. Further, water supply in a grid (WA_i, m^3) was reallocated proportional to the grid-level population (pop_i) within the basin:

$$WA_i = \left(pop_i / \sum_{i=1}^{n} pop_i \right) * Q, \tag{3}$$

Because the actual water resources quota in a grid cell also depended on water availability of the grid cell which consisted of local water resources of the grid cell and water from upstream of the grid cell, actual water supply under AIWAM must follow several constraints. Firstly, the AIWAM were implemented based on the river channel, i.e. the DDM30 river network (Döll and Lehner, 2002), which indicates water flow directions from upstream and downstream areas. Then, inter-basin water transfer was not considered here, and water resources were not allowed to be transferred from downstream to the upstream areas. Thus, the sum of actual water supply in a grid cell (WA_i) and its upstream grid cells (WA_{up}, m^3) must be lower than the sum of water availability in corresponding grid cells:

$$WA_i \le R_i + R_{up} - WA_{up}, \tag{4}$$

where R_i and R_{up} were water availability in grid i and its upstream grid cells, respectively. Additionally, actually water supply was lower than the total water demand. If actual local water supply (WA_i) was larger than local water demand (WD_i), the remaining outflow from this grid cell (Q_{out}, m^3) could be used for downstream areas. A detailed example of calculating water availability under AIWAM was shown in Supplementary Fig. S1.

This study adopted the future gridded population dataset under the SSP2 scenario from NCAR's integrated assessment model (IAM) group and the City University of New York Institute for Demographic Research to make AIWAM. These global spatially explicit population datasets (available at http://www.cgd.ucar.edu/iam/modeling/spatial-population-scenarios.html), which were developed using a gravity-type model parameterized to reflect the spatial patterns prescribed by each SSP, were quantitatively consistent with national population and urbanization projections in the SSP narratives (Jones and O'Neill, 2016). These population datasets, which cover the period 2010–2100 in a ten-year time step at a spatial resolution of 1/8-degree, were transferred to half-degree and annual scale by linear interpolation in this study.

2.5. Water scarcity assessment

Water scarcity by different sectors may affect different socioeconomic aspects. For example, water deficit in agriculture leads to losses in crop production, and water scarcity in nonagricultural sectors (i.e. domestic and industrial) may affect human daily life and industrial productions. Previous studies mostly used the water stress index (WSI) defined as the ratio of local total water demand to water availability, to represent water scarcity conditions (Vörösmarty et al., 2000; Wada et al., 2011; Mekonnen and Hoekstra, 2016; Veldkamp et al., 2017; Sun et al., 2019), without differentiating water scarcity for different sectors. Inter-sectoral water allocation priority was mostly determined by development goals, and varied across basins and countries (Molle and Berkoff, 2009). For example, water resources were first supplied to domestic and environmental sectors in USA (Brown, 2000). In Euphrates and Tigris Basin, Indus river basin, Pearl River basin, water allocation priorities varied with the development goals of local governments (Molle and Berkoff, 2009; Yan et al., 2018). However, so far, it is difficult to collect water allocation priorities of all basins of the world, particularly in transboundary basins where allocation priorities would be more complex. Thus, the integrated assessment models (IAMs) and large-scale hydrological models have implemented water allocation priorities among economic sectors in different ways. For example, GCAM model reconciled agricultural, energy, and industrial and municipal sector water demand with water availability in 235 river basins at an annual time step, based on relative prices and price-induced demand reduction (Kim et al., 2016). But some physical based global hydrological model could not consider the feedback of the economic decisions on water allocation, and they often assumed commonly used water allocation priorities. For example, the IMPACT model gave priority to domestic, industry, and livestock water uses before irrigation (Rosegrant et al., 2012), and H08 model prioritized municipal and industrial water abstraction over irrigation water (Hanasaki et al., 2013b). This water allocation priority was also widely used in previous global and regional water scarcity assessment (Elliott et al., 2014; Yin et al., 2017). To addressing SDG6, this study used the common used water allocation priority and assumed that the nonagricultural sectors (i.e. domestic and industrial water demands) had a higher priority over the agricultural water demand, that is, water was supplied to agriculture after domestic and industrial water supplies were met. Hence, water supplies to different sectors were calculated as follows:

$$\mathrm{WS}_{\mathrm{nonagr}} = \min\ (\mathrm{WD}_{\mathrm{ind}} + \mathrm{WD}_{\mathrm{dom}}, \mathrm{WA}); \tag{5}$$

$$\mathrm{WS}_{\mathrm{iagr}} = \max\,(\mathrm{WA} - \mathrm{WD}_{\mathrm{ind}} - \mathrm{WD}_{\mathrm{dom}}, 0); \tag{6}$$

where $\mathrm{WS}_{\mathrm{nonagr}}$ and $\mathrm{WS}_{\mathrm{agr}}$ were available water supplies to nonagricultural sectors and agricultural sector, respectively (m^3); $\mathrm{WD}_{\mathrm{dom}}$ and $\mathrm{WD}_{\mathrm{ind}}$ were water demands for domestic and industrial sectors, respectively (m^3); WA was the total available water resources to humans in a given grid cell (m^3).

Sectoral water deficit was used as an indicator to evaluate sectoral water scarcity conditions (Bijl et al., 2018; Flörke et al., 2018). This indicator was defined as the difference between sectoral water supply and water demand, which was calculated as follows:

$$\mathrm{DEF}_{\mathrm{nonagr}} = \max\ (\mathrm{WD}_{\mathrm{ind}} + \mathrm{WD}_{\mathrm{dom}} - \mathrm{WS}_{\mathrm{nonagr}}, 0); \tag{7}$$

$$\mathrm{DEF}_{\mathrm{agr}} = \max\ (\mathrm{WD}_{\mathrm{agr}} - \mathrm{WS}_{\mathrm{agr}}, 0); \tag{8}$$

where $\mathrm{DEF}_{\mathrm{nonagr}}$ and $\mathrm{DEF}_{\mathrm{agr}}$ were water deficit for nonagricultural sectors and agricultural sector, respectively (m^3); $\mathrm{WD}_{\mathrm{agr}}$ was water demand for agricultural sector (m^3). A 0 value of water deficit indicated that water demand was fully met, and positive value of water deficit meant severe water scarcity conditions. Thus, this study isolated water scarcity for agricultural and nonagricultural sectors.

Previous studies often defined population exposed to water scarcity in a grid cell as the total population living in the cell with water deficit (Mekonnen and Hoekstra, 2016; Veldkamp et al., 2017). However, this approach may over-estimate population exposed to water scarcity because the whole population in a grid cell was not necessarily exposed to water scarcity due to different magnitudes of water scarcity. For example, people would suffer different magnitudes of drinking water shortage with different domestic water deficit volumes. Going beyond previous studies, this study used the absolute population and irrigation cropland area exposed to water scarcity to characterize the socioeconomic consequences for nonagricultural and agricultural water scarcity, respectively. The absolute population and irrigation cropland area exposed to water scarcity were calculated as follows. Firstly, relative water deficit was calculated as the ratio of water deficit to sector water demand (Bijl et al., 2018):

$$D^{rel_{nonagr}} = \mathrm{DEF}_{\mathrm{nonagr}}/(\mathrm{WD}_{\mathrm{ind}} + \mathrm{WD}_{\mathrm{dom}}) * 100\%; \tag{9}$$

$$D^{rel_{agr}} = \mathrm{DEF}_{\mathrm{agr}}/\mathrm{WD}_{\mathrm{agr}} * 100\%; \tag{10}$$

where D^{rel}_{nonag} and D^{rel}_{agr} were relative water deficit for nonagricultural and agricultural sectors, respectively (%). Further, this study defined absolute population exposed to water scarcity ($\mathrm{pop}_{\mathrm{stress}}$)as the product of the total population ($\mathrm{pop}_{\mathrm{total}}$)in the grid cell and relative water deficit for nonagricultural sectors:

$$pop_{scarcity} = D^{rel}{}_{nonagr} * pop_{total}. \tag{11}$$

Similarly, the agricultural water scarcity indicator, i.e. irrigated cropland area exposed to water scarcity ($\mathrm{irrland}_{\mathrm{stress}}$, km^2) was calculated as:

$$irrland_{scarcity} = D^{rel}{}_{agr} * irrland_{total}, \tag{12}$$

where $irrland_{tot}$ was the total irrigated cropland area in the grid cell (km^2). If no water scarcity occurred in this grid cell, the values of $\mathrm{pop}_{\mathrm{stress}}$ and $\mathrm{irrland}_{\mathrm{stress}}$ both equaled 0.

2.6. Simulation with and without AIWAM

Two simulations were designed in this study to assess the effects of AIWAM on water scarcity assessment (Fig. 1). These two simulations both assessed global sectoral water scarcity at 0.5° × 0.5° grid resolution on an annual basis during 2020–2050, but they calculated water availability in different manners. Water availability in the first simulation, namely AIWAM, was calculated by applying the rule that the grid cell with high population would have high water use priority. It was an amendment to the widely used method in water scarcity assessment that set the upstream areas to have the higher priority to use the streamflow. The second simulation (namely NOAIWAM) was a sensitivity analysis, and assumed that the upstream water use was in the first priority, that is, upstream water availability was firstly used to meet local water demand. Hence, water availability for a grid i in NOAIWAM ($WA2_i$) was calculated as:

$$WA2_i = R_i + \sum_{i=1}^{k} q_{outk}, \quad (13)$$

where outflow from upstream grid k (q_{outk}) was computed as the difference between its water availability (WA_k) and water demand (WD_k), and water would flow into downstream areas only when water in the upstream grids was larger than their local water demands:

$$q_{outk} = \max(WA_k - WD_k, 0). \quad (14)$$

Therefore, based on actual water availability estimated by these two simulations (i.e. AIWAM and NOAIWAM), together with sectoral water demands (both agricultural and nonagricultural), global sectoral water scarcity was assessed at 0.5° × 0.5° spatial resolution during 2020–2050. When comparing sectoral water deficits as well as absolute population and irrigated land exposed to water scarcity between AIWAM and NOAIWAM, the effects of AIWAM on sectoral water scarcity assessment could be analyzed. An example of how to calculated sectoral water scarcity under these two simulations was shown in detail in Supplementary Fig. S1.

Climate projections from five GCMs were used to force the five GHMs, and thus 25 combinations of water availability projections and agricultural water demand were obtained. We then conducted 25 runs of global water scarcity assessments under both AIWAM and NOAIWAM. The ensemble medians across them were used to represent the results, and the interquartile range, i.e., the range between 25th and 75th percentiles, was also calculated to present the spread across multi-model ensembles.

3. Results

3.1. Spatial and temporal changing patterns of future global sectoral water scarcity

Fig. 2 shows the spatial distribution of global water deficit by sectors in 2050 under AIWAM. Due to limited precipitation and huge water demand by nonagricultural sectors, a large water deficit (>100 million m^3/yr per grid cell) for nonagricultural sectors is found in arid and semi-arid regions with population concentrations, such as the North China, the northern India, and some areas in the western USA. Moderate water deficit (2–100 million m^3/yr per grid cell) for nonagricultural sectors mainly occurs in northeastern China, the western coast of the Arabian Peninsula, and some areas in western Asia. Furthermore, in spite of low population density, low water deficit (<2 million m^3/yr per grid cell) can be also found in the Mongolian Plateau, Northern Africa, Mexico, the western coast of South America and the Orange River basin in South Africa. As for agricultural sector (shown in Fig. 2(b)), significant water scarcity is mainly found in arid and semi-arid regions where local precipitation cannot meet crop water demand for maximum food production. For example, in some areas of the Middle East and Central Asia, agricultural water demand would continually increase as the expansion of future irrigated cropland to meet increasing food demand, leading to severe water scarcity conditions for agricultural production. In the North China, Northern India, and Western USA, limited available surface water resources and large irrigation water demand are responsible for the large agricultural water deficit (Supplementary Fig. S2). In general, high total water deficit (as a sum of agricultural and nonagricultural water deficit) appears to occur in areas with large water demand, i.e. either large irrigated agriculture areas (e.g. the High Plain in the US and North coast of Africa) or dense population (e.g. large cities in the Western US and Bulgaria), or both of them (e.g. India, the North China plain, Central Asia and the Arabian Peninsula, see Fig. 2(c)). Furthermore, local water scarcity also occurs due to low surface water availability, e.g. in Sahara and the Mongolian Plateau (Supplementary Fig. S2).

Considering the effects of future climate change and socioeconomic development (Table 1), global total water deficit based on AIWAM is projected to increase by 48.3% from 2186.3 km^3/yr in 2020 to 3241.9 km^3/yr in 2050, with nonagricultural increasing from 296.2 km^3/yr in 2020 to 540.6 km^3/yr in 2050 (by 82.5%) and agricultural water deficit increasing from 1890.1 km^3/yr in 2020 to 2701.3 km^3/yr in 2050 (by 42.9%). At the regional level, total water deficits for all sectors show a significant increasing trend in all regions. Water deficit in some developing and arid regions shows a large increasing trend (e.g. Middle East, Central Asia, and Northern Africa) where available water resources cannot meet increasing human water demand, and human water demand would significantly increase due to population growth and increasing energy and food production (Supplementary Fig. S2). For example, total water deficit in Central Asia and Middle East will increase by 148% and 105% during 2020–2050, respectively (Table 2). In contrast, in some developed regions (e.g. Western Europe, North America, and Oceania), total water deficit shows a slight or moderate increasing trend as a result of low population growth and improving water-saving techniques. For example, in spite of a reduced total water demand in USA, a decrease of water availability in the western USA leads to a moderate increase of total water deficit (by about 20%). As for the changing pattern of sectoral water deficit at regional level, both nonagricultural and agricultural water deficits would increase continuously during 2020–2050 in most regions. However, nonagricultural water deficit in regions like North America, Northern Africa and Middle East would first increase from 2020 to 2040, and then decrease after 2040. In contrast, agricultural water deficit also would keep decreasing after 2040 in Eastern and Western Africa, as well as Southern and Southeastern Asia (Supplementary Table S3).

Global population and irrigated cropland area exposed to water scarcity were also estimated (Fig. 3 and Table 2). As shown in Fig. 3, about 0.75 billion population and 0.86 million km^2 irrigated cropland in the world would be exposed to water scarcity in 2020 under AIWAM. Areas with large numbers of population exposed to water scarcity in 2020 are mainly found in North America (95.5 million, mostly in the western US), Northern Africa (59.1 million), Eastern Asia (295.8 million, mostly in Northern China), Southern Asia (132.3 million, mostly in Pakistan) and Middle East (63.6 million). Irrigated cropland areas exposed to water scarcity are mainly found in Eastern Asia (0.27 million km^2), Southern Asia (0.36 million km^2) and the Middle East (0.07 million km^2). Furthermore, the number of population and size of irrigated cropland area exposed to water scarcity would increase by about 70.4% and 25.3%, respectively, in 2050 compared with that in 2020, indicating that future climate and socioeconomic development would greatly aggravate global water scarcity. Both population and irrigated cropland areas under water scarcity would increase continuously during 2020–2050 in most regions (Supplementary Table S4). Hotspot regions with significantly aggravated water scarcity during 2020–2050 are mainly found in Northern Africa (with population and irrigated cropland area exposed to water scarcity increased by 40% and 79%, respectively), Central Asia with population and irrigated cropland area exposed to water scarcity increased by 62% and 95%, respectively) and the Middle East (with population and irrigated cropland area exposed to water scarcity increased by 78% and 86%, respectively).

3.2. The role of AIWAM on global sectoral water scarcity assessment

Global water deficit for nonagricultural sectors decreases by about 8.8% in 2050 when considering AIWAM compared with NOAIWAM (593 km^3/yr in NOAIWAM versus 541 km^3/yr in AIWAM), while water deficit for agricultural sector increases about 40.9 km^3/yr by 1.5% (Table 2). Furthermore, water deficit for nonagricultural sectors in NOAIWAM is higher than that in AIWAM across most regions, especially

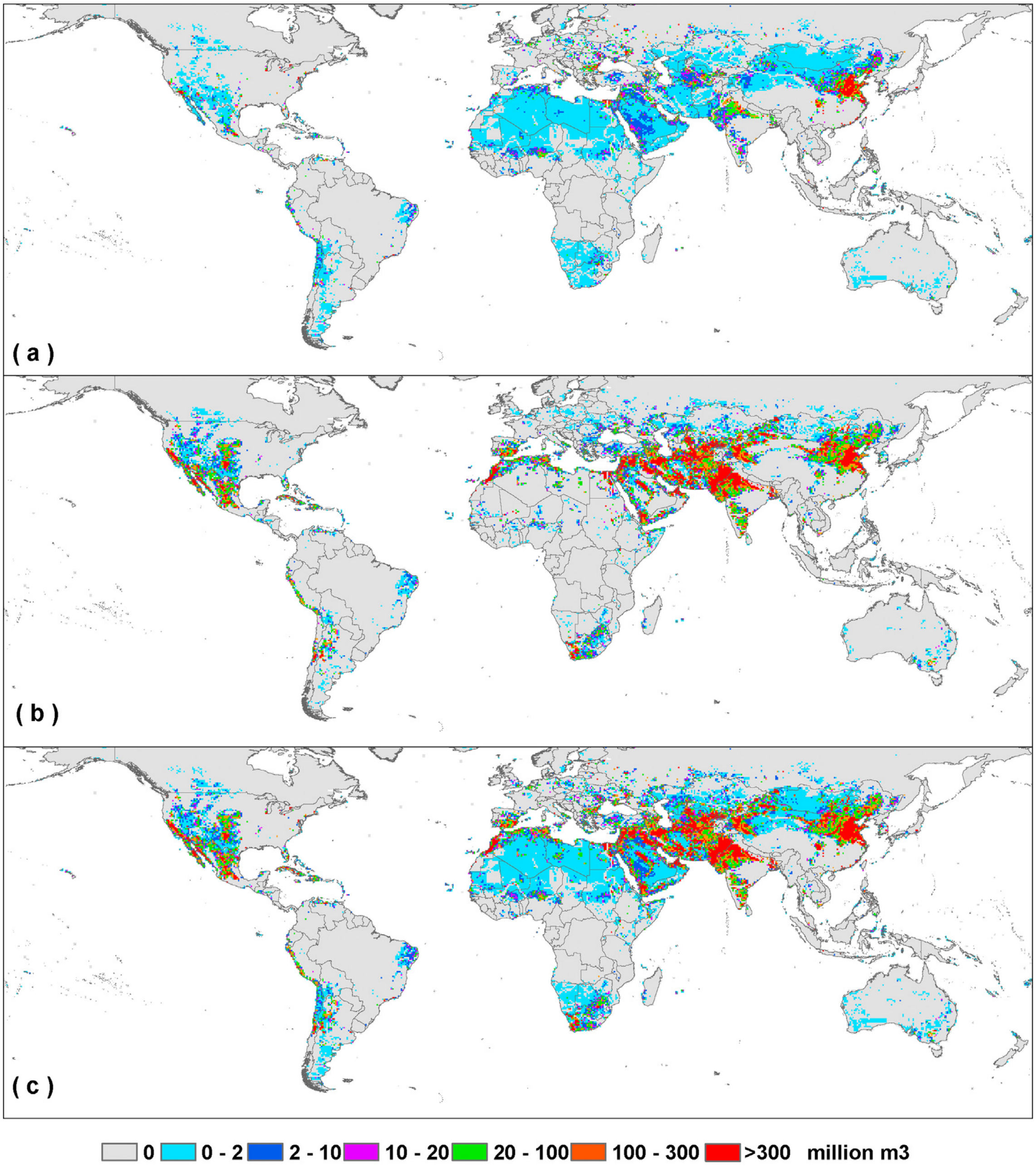

Fig. 2. The spatial pattern of global water deficit by sectors at global $0.5 \times 0.5°$grid scale in 2050 with consideration of AIWAM: (a) water deficit for nonagricultural sectors, (b) water deficit for agricultural sector, and (c) total water deficit. The results were the ensemble-median values across these 25 simulations.

in Southern Asia, the Middle East and Central Asia, indicating that water scarcity for nonagricultural sectors is greatly mitigated by AIWAM. Conversely, water deficit for agricultural sector might increase if AIWAM are adopted. Fig. 4 shows the difference of sectoral water deficit between AIWAM and NOAIWAM at the grid level in 2050, where a negative value represents sectoral water scarcity mitigation by AIWAM and a positive value indicates sectoral water scarcity aggravation. For nonagricultural sectors (Fig. 4(a)), a decrease of water deficit (over 5 million m^3) is found in areas with high population density, such as downstream of the Yellow River basin, the Hai River basin, the Indus River basin, as well as some areas in Western US.

Further, some areas with water deficit for nonagricultural sectors in NOAIWAM (e.g. the downstream of the Yellow River basin and the Indus River basin, some areas in the western China and western US) would no more suffer water scarcity when AIWAM is adopted (shown in Supplementary Fig. S3). In terms of agricultural sector, AIWAM leads to a significant increase of water deficit in Western US, Morocco, Northeastern China, the upstream of the Yellow River basin, and the Indus River basin and the Euphrates and Tigris River basin, and some of these areas would even move into water scarcity for agriculture (Fig. 4(b) and Supplementary Fig. S3), because part of available water resources in these areas is reallocated to nonagricultural water demand in the downstream areas. For example, in the Yellow River basin, 70% of population resides in the middle and lower sub-basins which only accounts for 32% of total area and 29% of total runoff of the whole basin (YRCC, 2013; Yin et al., 2017). When taken AIWAM into account, more available surface water resources are reallocated to downstream areas with large population to mitigate water scarcity conditions for nonagricultural sectors. As a result, the water deficit for nonagricultural sectors decreases by about 28% (Fig. 5), but water scarcity for agriculture in the

Table 1
Water deficit by sectors under two simulations (i.e. AIWAM and NOAIWAM) for the years 2020 and 2050 across global regions, which were the ensemble-median values across these 25 simulations. The areas of these 16 regions are shown in Supplementary Fig. S4.

	Water deficit for nonagricultural sectors (km^3/yr)				Water deficit for agricultural sector (km^3/yr)			
	AIWAM		NOAIWAM		AIWAM		NOAIWAM	
	2020	2050	2020	2050	2020	2050	2020	2050
Oceania	0.3	0.6	0.3	0.6	3.8	3.7	3.8	3.6
Central America and Caribbean	0.1	0.3	0.1	0.3	6.7	9.3	6.7	9.3
North America	59.0	64.4	62.1	68.0	151.9	192.8	148.9	189.1
South America	13.1	21.7	13.8	22.7	37.6	43.8	36.7	42.7
Eastern Africa	0.3	1.9	0.3	1.9	12.2	13.3	12.2	13.2
Northern Africa	10.4	13.4	10.7	13.9	127.0	195.7	126.6	195.4
Southern Africa	2.6	6.0	2.7	6.3	47.0	59.3	46.9	59.1
Western Africa	0.7	5.5	0.7	5.5	9.6	12.3	9.6	12.3
Central Europe	8.4	16.7	8.4	16.6	1.3	4.3	1.3	3.3
Eastern Europe	18.7	32.2	18.7	32.2	4.2	9.4	4.2	9.1
Western Europe	3.2	3.2	3.7	3.5	17.9	18.7	17.5	18.3
Central Asia	14.0	28.1	15.2	32.8	103.2	267.3	101.7	260.3
Eastern Asia	126.0	272.6	138.3	291.8	294.8	375.3	282.5	354.9
Southern Asia	14.8	43.3	19.2	52.6	752.5	821.9	746.4	812.3
Southeastern Asia	3.3	9.3	3.3	9.3	2.7	2.4	2.7	2.3
Middle East	22.7	21.2	25.4	28.9	326.1	692.2	322.1	683.1
Global	296.2	540.6	322.8	592.7	1890.1	2701.3	1864.8	2660.4

upstream areas becomes severer. Similar situations are also found in the Indus River basin and the Euphrates and Tigris River basin, where water deficits for nonagricultural sectors decrease by about 41% and 50%, respectively.

In terms of global absolute population and irrigated cropland area exposed to water scarcity by AIWAM and NOAIWAM during 2020–2050, AIWAM would mitigate water scarcity for nonagricultural sectors, and lead to 0.15 (0.13–0.16) billion of global population no more suffering water scarcity, which, however, at the cost of driving 0.031 (0.027–0.038) million km^2 more irrigated cropland area faced water scarcity in 2050 (Fig. 3). Using AIWAM, population exposed to water scarcity decreases by about 12%, while irrigated cropland area exposed water scarcity increases about 6% in 2050. Furthermore, population that no more suffer water scarcity is mainly identified in North America (8.6 million), Eastern Asia (29.6 million), Southern Asia (66.6 million), and Middle East (20.8 million); while irrigated cropland areas suffering aggravated water scarcity is mainly found in Central Asia (6020 km^2), Eastern Asia (8090 km^2), Southern Asia (6890 km^2), and Middle East (4260 km^2) (Table 2). In addition, the effects of AIWAM on global water scarcity conditions would be enhanced along with climate change and socioeconomic development.

Specially, the absolute population and irrigated cropland area exposed to water scarcity in 2050 for major basins were compared between two simulations (Fig. 6). For basins under severe water scarcity conditions, e.g. the Yellow River basin, the Indus river basin, and the Euphrates and Tigris River basin, where local water availability is not able to meet the large water demand, AIWAM would reallocate water to areas with dense population, resulting in a significant reduction of population exposed to water scarcity by shifting water supply from agricultural to nonagricultural uses. However, in some humid regions, such as the Yangtze River basin and the Mississippi River basin, AIWAM do not have a significant effect on water scarcity condition.

Table 2
Population and irrigated cropland area exposed to water scarcity under two simulations (i.e. AIWAM and NOAIWAM) for the years 2020 and 2050 across global regions. The results were the ensemble-median values across these 25 simulations. The areas of these 16 regions are shown in Supplementary Fig. S4.

	Population exposed to water scarcity (million)				Irrigated cropland area exposed to water scarcity (1000 km^2)			
	AIWAM		NOAIWAM		AIWAM		NOAIWAM	
	2020	2050	2020	2050	2020	2050	2020	2050
Oceania	1.0	2.4	1.0	2.5	6.0	6.3	5.8	6.0
Central America and Caribbean	0.5	1.5	0.5	1.5	3.1	3.5	3.0	3.5
North America	95.5	126.2	100.9	134.7	40.9	52.9	38.8	51.5
South America	54.9	83.1	57.9	86.8	9.3	11.0	9.1	10.4
Eastern Africa	7.4	23.3	7.4	23.5	4.9	4.9	4.9	4.9
Northern Africa	59.1	83.0	61.1	86.8	29.3	52.4	29.0	52.1
Southern Africa	11.3	19.7	12.1	20.5	8.9	9.6	8.9	9.5
Western Africa	10.0	52.0	10.0	52.2	0.5	0.6	0.5	0.6
Central Europe	6.5	13.9	6.5	13.9	1.8	4.6	1.7	3.4
Eastern Europe	22.6	29.2	22.7	29.4	2.1	5.0	2.1	4.8
Western Europe	13.9	15.0	14.8	16.8	13.5	14.3	13.1	14.1
Central Asia	15.6	25.2	17.2	30.9	49.7	97.0	48.2	91.0
Eastern Asia	295.8	415.5	325.7	445.0	275.5	329.5	269.1	321.4
Southern Asia	132.3	301.7	180.9	368.3	363.0	386.1	359.5	379.2
Southeastern Asia	8.9	27.3	8.9	27.7	4.8	5.4	4.8	5.3
Middle East	63.6	113.5	75.2	134.2	71.8	133.7	70.3	129.4
Global	750.6	1279.2	857.6	1415.4	868.5	1088.6	848.7	1060.6

4. Discussion

4.1. Comparison with previous studies

The spatial pattern of global water scarcity in the future in this study agreed with previous water scarcity assessment, e.g. Wada et al. (2014) and Greve et al. (2018), with water scarcity mainly found in the areas with intensive irrigated cropland or dense population. For example, India, Northern China, the Middle East, and Mexico were highlighted as water scarcity hotspots across historical and future periods in all cases (Hanasaki et al., 2013b; Hejazi et al., 2014). Furthermore, in terms of changing patterns of future water scarcity, results from this study showed consistency to previous water scarcity projections (e.g. Schewe et al., 2014). As future population growth and socioeconomic development would greatly increase human water demand, water scarcity would increase significantly in most regions of the world, especially in developing regions. In addition, this study suggested that sectoral water scarcity would increase slightly or non-significantly in some developed regions, e.g. Oceania and Western Europe, which was also consistent with previous projections (Cui et al., 2018; Graham et al., 2020). However, it is difficult to conduct a detailed comparison of water scarcity projections due to differences in water scarcity metrics and methodologies in water scarcity assessment (Liu et al., 2017).

4.2. Limitations of this study

A few limitations of the methodologies, which may introduce uncertainties into water scarcity assessment, need to be taken into account in future analysis. Firstly, the human impacts on hydrological processes were not fully represented in this study. Water availability was simulated by GHMs regarding future climate change but without consideration of human impacts. Actually, human activities, e.g., human water use, human induced land use and land cover change and urbanization, would affect hydrological processes upstream and downstream to different degrees and further lead to changes in water availability (Veldkamp et al., 2017; Liu et al., 2019). Neglecting the impacts of human activities on future water availability would lead to uncertainties in water scarcity projection. Second, the AIWAM were not fully coupled into hydrological models, i.e., this study was based on off-line simulations. This largely limits the representation of the interactions among human activities regarding water withdrawal, e.g., the competition between different water users. The coupling of AIWAM with hydrological processes would improve the modeling of the interactions and might

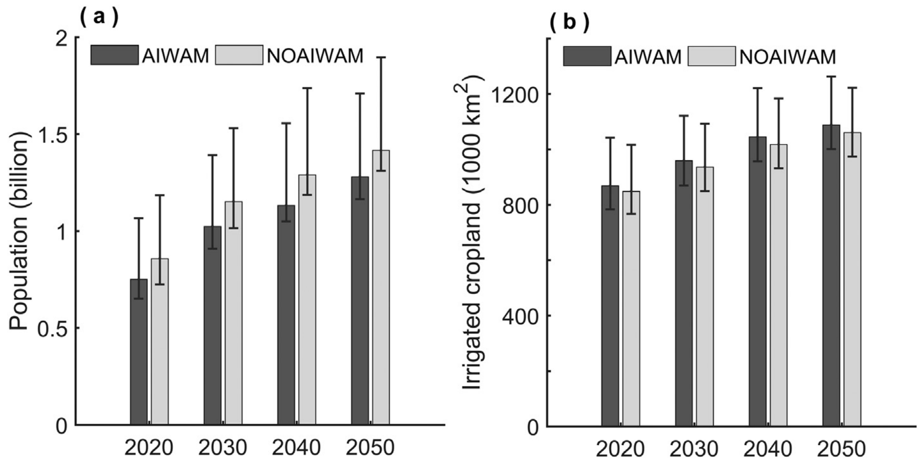

Fig. 3. Global (a) population and (b) irrigated cropland exposed to water scarcity under two simulations (i.e. AIWAM and NOAIWAM) during 2020–2050: The columns are ensemble-median values, and the uncertainties bar represents the interquartile range (q25-q75).

reshape the patterns of water scarcity in some regions. Then, the offline simulations make it difficult to include return flow (i.e., the part of water withdrawal returns to river channels) in the estimation of water availability. Although return flow was not fully available to humans, neglecting return flow in water scarcity assessment would result in lower water availability in downstream areas and overestimation of their water scarcity conditions (Munia et al., 2016). As this study only used water withdrawal (including agricultural, domestic and industrial sectors) to assess water scarcity, the use of both water withdrawal and water consumption in water scarcity assessment could provide important information. However, this study only used water withdrawal due to absence of water consumption dataset (Vanham et al., 2018).

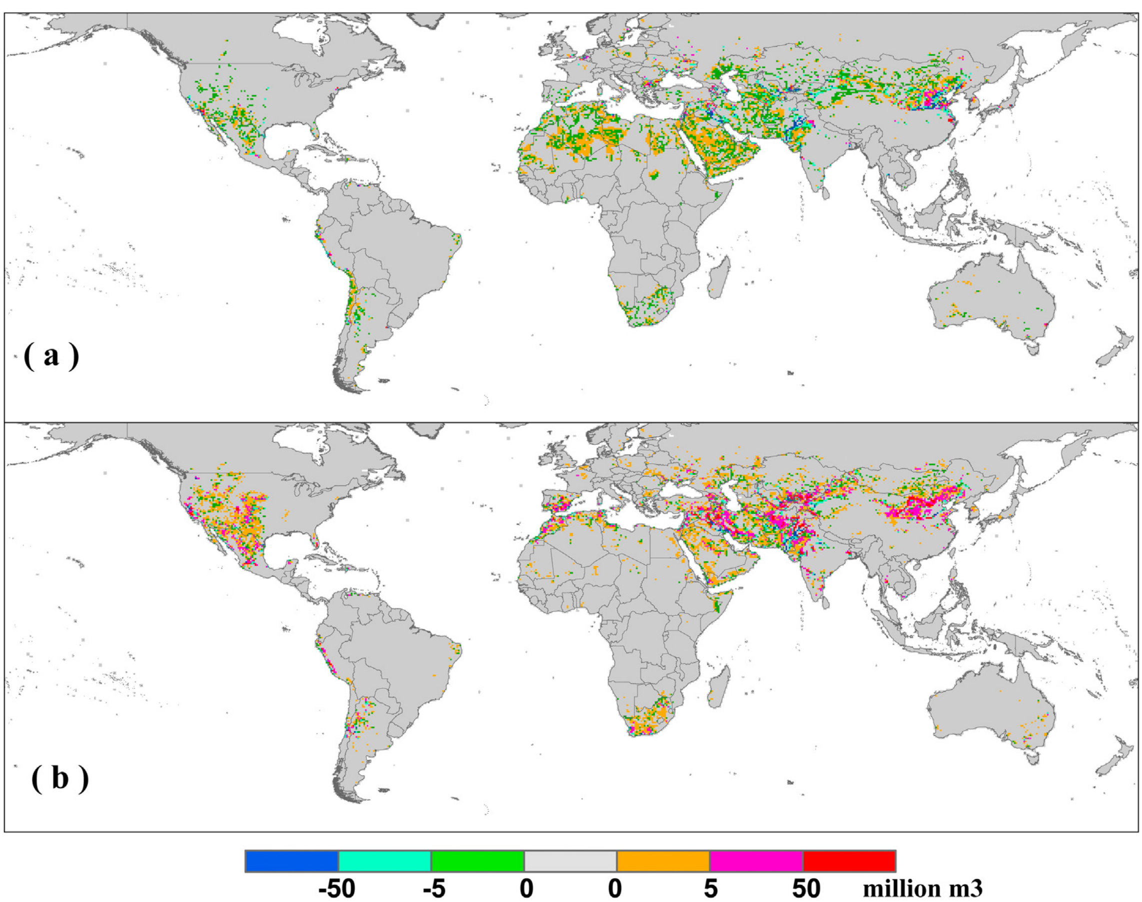

Fig. 4. Differences of sectoral water deficits between AIWAM and NOAIWAM (AIWAM minus NOAIWAM) in 2050 for (a) nonagricultural sectors and (b) agricultural sector. A negative value represents water scarcity mitigation by AIWAM and a positive value indicates sectoral water scarcity aggravation. The results were the ensemble-median values across these 25 simulations.

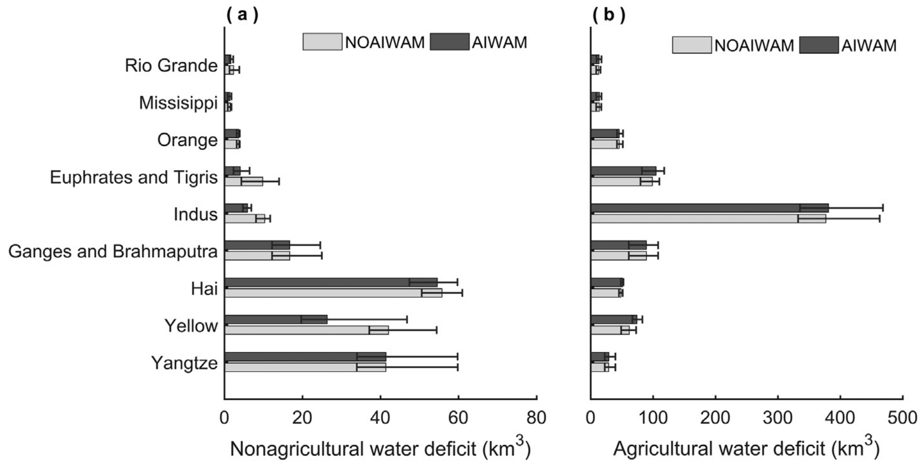

Fig. 5. Water deficits for global major basins in 2050 under two simulations (i.e. AIWAM and NOIAWAM) for (a) nonagricultural sectors and (b) agricultural sector. The columns are ensemble-median value, and the uncertainties bar represents the interquartile range (q25-q75). The location of these nine river basins is shown in Supplementary Fig. S5.

Furthermore, upstream human water uses would often affect water quality, which may reduce the available water resources in the downstream areas (Ma et al., 2020; Van Vliet et al., 2021). Neglecting the water quality aspect may result in an underestimation of downstream water scarcity (Liu et al., 2016; Jiang, 2009). Moreover, inter-basin water transfer was not considered in this study. As reported by Yin et al. (2020), the South to North Water Diversion project in China would significantly alleviate water scarcity in Northern China (particularly Beijing) and thus increase the agricultural production and have more economic benefits. The large cities often extend their water supply via inter-basin water transfer (Flörke et al., 2018). Thus, not taking into account inter-basin water transfer would lead to overestimation of water scarcity in water transfer destination and would underestimate water scarcity in source areas. The total runoff from the GHMs includes groundwater recharge and fast surface and subsurface runoff (Portmann et al., 2013). From the hydrological perspective, river flow and groundwater would recharge each other in different seasons (Huang et al., 2019b). Thus, the renewable groundwater dynamics has been reflected in the river flow and this study actually considered renewable water availability including both renewable surface water and groundwater in a long-term period for which groundwater and river flow recharges were balanced. However, in a short-term perspective (e.g., monthly), the explicit inclusion of groundwater recharge in water availability would reduce the uncertainty in water scarcity assessment. The nonrenewable groundwater was not explicitly considered due to a lack of related information, which may also lead to underestimation of water availability in regions that heavily rely on this water source. Nevertheless, it was noted that nonrenewable groundwater could only be unlimitedly pumped for a specific period but it is not a sustainable water source, thus, including it in water availability may underestimate water scarcity in these regions, e.g., North China and Northern India (Turner et al., 2019).

The strategy of AIWAM in this study aimed to move water away from agriculture to uses with higher economic value (i.e. nonagricultural sectors), and grid cell with high non-agricultural water demand (e.g. the populous areas) would have high water resources quota. In this study, AIWAM partly addressed the SDG 6 by reallocating water availability according to population density and setting a high priority for nonagricultural uses to mitigate water scarcity for nonagricultural sectors. However, the uniform allocation priority in AIWAM may not be proper in some basins and thus may lead to uncertainty in water scarcity assessment. AIWAM would be useful in the basins with significant competition of water resources among sectors between upstream and downstream, e.g., the Yellow River basin, the Hai River basin and

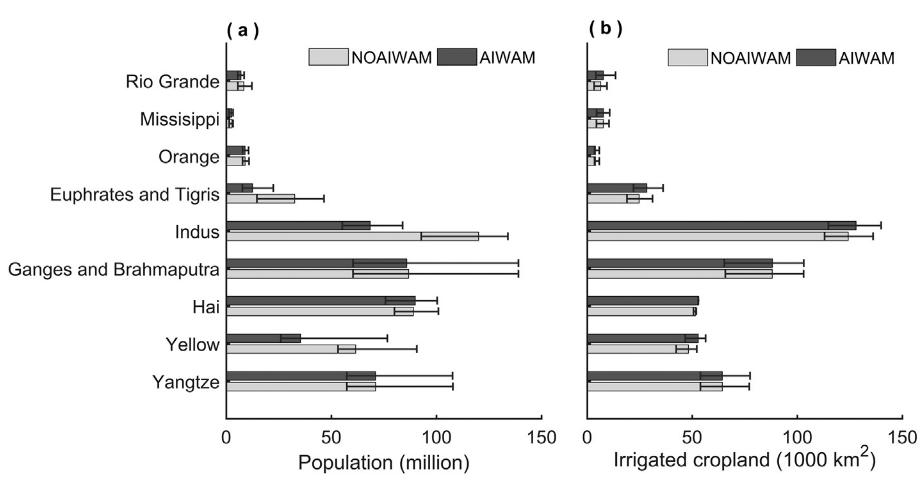

Fig. 6. Comparison of (a) population and (b) irrigated cropland area exposed to water scarcity under two simulations (i.e. AIWAM and NOIAWAM) for global major basins in 2050. The columns are ensemble-median values, and the uncertainties bar represents the interquartile range (q25-q75). The locations of these nine river basins is shown in Supplementary Fig. S5.

the Indus River basin. More and high-quality water availability for human life is an essential goal in these basins. The high priority of industrial water use in AIWAM may not be applicable in some regions, e.g., in European countries and USA, where industrial water use may have a relatively low priority (Molle and Berkoff, 2009). This assumption may be not the reality for some basins (particularly transboundary ones) where agricultural water use has a high priority over downstream nonagricultural water demands. Thus, various priority of water uses between upstream and downstream and among sectors across global basins and countries should be considered in AIWAM in the future studies, which may also improve the feasibility over the world.

4.3. Implications

This study projected future global water scarcity conditions during 2020–2050 and provided insights on the effects of AIWAM on global water scarcity over time, which was of great significance for both revealing mechanisms behind water scarcity and decision making. The water scarcity assessment with AIWAM provides a scenario analysis that shows the tradeoff between nonagricultural and agricultural water scarcity across downstream and upstream areas by reallocating water resources between sectoral water demands.

In this study, available water resources were reallocated to areas with large population. AIWAM would alleviate global water scarcity for nonagricultural sectors, but in turn aggravate global water scarcity for agricultural sector. Although the AIWAM appeared different to represent water allocation practices in the real world case, the results were useful in guiding the water management policy to cope with future increasing water scarcity conditions. Mitigation in nonagricultural water scarcity in the downstream area would achieve more economic benefit as agriculture water use was usually inefficient both in technical (it incurs many losses) and economic terms (water productivity is low). Aggravation in agricultural water scarcity in the upstream area would promote the design and provision of mechanisms to compensate farmers for losses and deprivation, as well as development of water conservancy facilities, such as or desalination or inter-basin water transfer projects (e.g. the South to North Water Diversion project in China). Recent studies have showed that decreased irrigation water use intensity have widespread slowdown of the growth rates of agricultural water use in China (Zhou et al., 2020). However, this study did not consider water use efficiency improvement. AIWAM lead to aggravated water scarcity in agricultural sector in this study, which implies that sectoral water use competition would pose great challenges for meet agriculture water use, and regions with agricultural water use constraints are encouraged to explore options to reduce water use intensity of irrigation in the future investigation, e.g., scenarios of higher water use efficiency to achieve universal access to affordable water resource in all sectors and better integrated agricultural water management for reducing agricultural water scarcity.

The AIWAM has been employed in water resources allocation in previous literatures. For example, in the Yellow River basin, water managers implemented a flow regulation rule that reduced upstream irrigation water abstraction in order to guarantee the nonagricultural water supply in the downstream areas (Cai and Rosegrant, 2004; Yin et al., 2017). Water resources were first allocated to meet water demand from domestic and environmental requirements in the USA (Brown, 2000). Different inner-basin water allocation measures were adopted by the local governments according to the development goals in the Euphrates and Tigris Basin, the Indus river basin, and the Pearl River basin (Molle and Berkoff, 2009; Yan et al., 2018). For these areas where inner-basin water allocation measures have been already adopted, the AIWAM in this study could provide a reference for coping with future water scarcity, and the government would improve the ongoing inner-basin water allocation measures under future changing environment and development goals. In addition, some areas haven't applied the inner-basin water allocation measures, leading to upstream-downstream conflicts, especially in a few transboundary basins. Limitless upstream water use would exacerbate downstream water scarcity conditions in a few transboundary basins, which may further lead to serious conflicts (Munia et al., 2018), and the competition of water use between upstream and downstream areas would more serious under future changing environment (Munia et al., 2020). Therefore, the AIWAM could provide a useful strategy to improve international cooperation as well as the adaptation to future water scarcity, and further avoid potential upstream-downstream conflicts. In general, the findings in this study reflected the competition of water use between upstream and downstream among sectors, and in this case, serve as a scenario for a trade-off analysis of meeting the nonagricultural water uses within a basin from. Thus, the AIWAM in this study can provide a reference for water scarcity assessment and water management with human adaptations in the future a precautionary perspective when both agricultural and nonagricultural water uses are projected to increase worldwide.

5. Conclusions

In this study, AIWAM was incorporated into future global water scarcity assessment. The results show that future water scarcity would mainly occur in arid and semi-arid areas with either large irrigated cropland (e.g. the High Plain in the US and North coast of Africa) or dense population (e.g. large cities in the Western US and Bulgaria), or both of them (e.g. India, the North China Plain, Central Asia and Arabian Peninsula). Future climate change and socioeconomic development would aggravate global water scarcity. The global water deficit is likely to increase by 48.3% during 2020–2050, and the number of absolute population and irrigated cropland area exposed to water scarcity in 2050 are projected to increase by 82.5% and 42.9%, respectively, in comparison to those in 2020. It is found that the adaptive measures that reallocate water resources in the river basin would mitigate water scarcity for nonagricultural sectors, particularly in the downstream areas with intensive population. AIWAM result in a decrease by 12% of global population exposed to water scarcity in 2050 when compared with that without the consideration of AIWAM. At the same time, the adaptive measures might intensify agricultural water scarcity in the upstream of these basins. This study emphasized the importance of considering AIWAM in water scarcity assessment under future climate change. The findings in this study would be helpful in developing policies to reduce population exposure to water scarcity and achieve the goals of sustainable water management.

Data availability

The future runoff simulation and water demand for nonagricultural sectors are obtained from the Inter-Sectoral Impact Model Intercomparison Project coordinating team (https://www.isimip.org/). Future population dataset is available at http://www.cgd.ucar.edu/iam/modeling/spatial-population-scenarios.html. Future agricultural water demand was obtained from (Huang et al., 2019a), and the authors will provide the data on request.

CRediT authorship contribution statement

Zhongwei Huang: Conceptualization, Methodology, Software, Writing – original draft. **Xingcai Liu:** Writing – review & editing. **Siao Sun:** Writing – review & editing. **Yin Tang:** Writing – review & editing. **Xing Yuan:** Writing – review & editing. **Qiuhong Tang:** Conceptualization, Writing – review & editing.

Declaration of competing interest

The authors declare that they have no known competing financial interests or personal relationships that could have appeared to influence the work reported in this paper.

Acknowledgments

This research was supported by the National Natural Science Foundation of China (Grant Nos. 41790424, 41730645 and 41425002), the Strategic Priority Research Program of the Chinese Academy of Sciences (XDA20060402), the General Subject of Colleges and Universities Natural Science Foundation of Jiangsu Province (20KJB170026), Newton Advanced Fellowships, and the Startup Foundation for Introducing Talent of NUIST (2019r080, 2018r078). We thank the Inter-Sectoral Impact Model Inter-comparison Project coordinating team for providing the multi-model simulations.

Appendix A. Supplementary data

Supplementary data to this article can be found online at https://doi.org/10.1016/j.scitotenv.2021.146973.

References

Barnett, J., Rogers, S., Webber, M., Finlayson, B., Wang, M., 2015. Sustainability: transfer project cannot meet China's water needs. Nature 527 (7578), 295.
van Beek, L., Wada, Y., Bierkens, M.F., 2011. Global monthly water stress: 1. Water balance and water availability. Water Resour. Res. 47 (7).
Bijl, D.L., Biemans, H., Bogaart, P.W., Dekker, S.C., Doelman, J.C., Stehfest, E., van Vuuren, D.P., 2018. A global analysis of future water deficit based on different allocation mechanisms. Water Resour. Res. 54, 5803–5824. https://doi.org/10.1029/2017WR021688.
Biswas, A.K., 2004. Integrated water resources management: a reassessment. Water Int. 29, 248–256. https://doi.org/10.1080/02508060408691775.
Brown, L.R, 2000. How water scarcity will shape the new century. Keynote Speech presented at Stockholm Water Conference August 14, 2000.
Cai, X., Rosegrant, M.W., 2004. Optional water development strategies for the Yellow River Basin: balancing agricultural and ecological water demands. Water Resour. Res. 40 (8).
Calvin, K., Wise, M., Kyle, P., Patel, P., Clarke, L., and Edmonds, J. (2014), Trade-offs of different land and bioenergy policies on the path to achieving climate targets. Clim. Chang., 123(3–4), 691–704.
Calvin, K., Patel, P., Clarke, L., Asrar, G., Bond-Lamberty, B., Di Vittorio, A., Edmonds, J., Hartin, C., Hejazi, M., Iyer, G., Kyle, P., Kim, S., Link, R., McJeon, H., Smith, S.J., Waldhoff, S., Wise, M., 2018. GCAM v5.1: representing the linkages between energy, water, land, climate, and economic systems. Geosci. Model Dev. 1-37. https://doi.org/10.5194/gmd-2018-214.
Chang, I.S., Zhao, M., Chen, Y., Guo, X., Zhu, Y., Wu, J., Yuan, T., 2020. Evaluation on the integrated water resources management in China's major cities–based on City Blueprint® Approach. J. Clean. Prod. 262, 121410.
Chaturvedi, V., Hejazi, M., Edmonds, J., Clarke, L., Kyle, P., Davies, E., Wise, M., 2015. Climate mitigation policy implications for global irrigation water demand. Mitig. Adapt. Strateg. Glob. Chang. 20 (3), 389–407.
Chen, M., Vernon, C.R., Graham, N.T., Hejazi, M., Huang, M., Cheng, Y., Calvin, K., 2020. Global land use for 2015–2100 at 0.05° resolution under diverse socioeconomic and climate scenarios. Scientific Data 7 (1), 1–11.
Cheng, H., Hu, Y., Zhao, J., 2009. Meeting China's Water Shortage Crisis: Current Practices and Challenges. ACS Publications.
Cui, R.Y., Calvin, K., Clarke, L., Hejazi, M., Kim, S., Kyle, P., Wise, M., 2018. Regional responses to future, demand-driven water scarcity. Environ. Res. Lett. 13 (9), 094006.
Döll, P., Lehner, B., 2002. Validation of a new global 30-min drainage direction map. J. Hydrol. 258 (1), 214–231. https://doi.org/10.1016/S0022-1694(01)00565-0.
Edmonds, J., Wise, M., Pitcher, H., Richels, R., Wigley, T., Maccracken, C., 1997. An integrated assessment of climate change and the accelerated introduction of advanced energy technologies-an application of MiniCAM 1.0. Mitig. Adapt. Strateg. Glob. Chang. 1 (4), 311–339.
Elliott, J., Deryng, D., Müller, C., Frieler, K., Konzmann, M., Gerten, D., Glotter, M., Flörke, M., Wada, Y., Best, N., Eisner, S., Fekete, B.M., Folberth, C., Foster, I., Gosling, S.N., Haddeland, I., Khabarov, N., Ludwig, F., Masaki, Y., Olin, S., Rosenzweig, C., Ruane, A.C., Satoh, Y., Schmid, E., Stacke, T., Tang, Q., Wisser, D., 2014. Constraints and potentials of future irrigation water availability on agricultural production under climate change. Proc. Natl. Acad. Sci. 111 (9), 3239–3244.
Ferguson, C.R., Pan, M., Oki, T., 2018. The effect of global warming on future water availability: CMIP5 synthesis. Water Resour. Res. 54, 7791–7819.
Flörke, M., Kynast, E., Bärlund, I., Eisner, S., Wimmer, F., Alcamo, J., 2013. Domestic and industrial water uses of the past 60 years as a mirror of socio-economic development: a global simulation study. Glob. Environ. Chang. 23 (1), 144–156.
Flörke, M., Schneider, C., McDonald, R.I., 2018. Water competition between cities and agriculture driven by climate change and urban growth. Nature Sustainability 1 (1), 51–58. https://doi.org/10.1038/s41893-017-0006-8.
Fricko, O., Havlik, P., Rogelj, J., Klimont, Z., Gusti, M., Johnson, N., Kolp, P., Strubegger, M., Valin, H., Amann, M., Ermolieva, T., Forsell, N., Herrero, M., Heyes, C., Kindermann, G., Krey, V., McCollum, D.L., Obersteiner, M., Pachauri, S., Rao, S., Schmid, E., Schoepp, W., Riahi, K., 2017. The marker quantification of the shared socioeconomic pathway 2: a middle-of-the-road scenario for the 21st century. Glob. Environ. Chang. 42, 251–267. https://doi.org/10.1016/j.gloenvcha.2016.06.004.
Gaaloul, N., Eslamian, S., & Katlane, R. (2020). Impacts of climate change and water resources management in the Southern Mediterranean Countries. Water Productivity Journal, 1(1), 51–72.
Gerten, D., Heinke, J., Hoff, H., Biemans, H., Fader, M., Waha, K., 2011. Global water availability and requirements for future food production. J. Hydrometeorol. 12 (5), 885–899.
Graham, N.T., Hejazi, M.I., Chen, M., Davies, E.G.R., Edmonds, J.A., Kim, S.H., Wise, M.A., 2020. Humans drive future water scarcity changes across all shared socioeconomic pathways. Environ. Res. Lett. 15 (1), 014007. https://doi.org/10.1088/1748-9326/ab639b.
Greve, P., Kahil, T., Mochizuki, J., Schinko, T., Satoh, Y., Burek, P., Fischer, G., Tramberend, S., Burtscher, R., Langan, S., Wada, Y., 2018. Global assessment of water challenges under uncertainty in water scarcity projections. Nature Sustainability 1 (9), 486–494. https://doi.org/10.1038/s41893-018-0134-9.
Hanasaki, N., Kanae, S., Oki, T., Masuda, K., Motoya, K., Shirakawa, N., Shen, Y., Tanaka, K., 2008a. An integrated model for the assessment of global water resources part 1: model description and input meteorological forcing. Hydrol. Earth Syst. Sci. 12 (4), 1007–1025. https://doi.org/10.5194/hess-12-1007-2008.
Hanasaki, N., Kanae, S., Oki, T., Masuda, K., Motoya, K., Shirakawa, N., Shen, Y., Tanaka, K., 2008b. An integrated model for the assessment of global water resources part 2: applications and assessments. Hydrol. Earth Syst. Sci., 1027–1037 https://doi.org/10.5194/hess-12-1027-2008.
Hanasaki, N., Fujimori, S., Yamamoto, T., Yoshikawa, S., et al., 2013a. A global water scarcity assessment under shared socio-economic pathways – part 1: water use. Hydrol. Earth Syst. Sci. 2393–2413.
Hanasaki, N., Fujimori, S., Yamamoto, T., Yoshikawa, S., Masaki, Y., Hijioka, Y., Kainuma, M., Kanamori, Y., Masui, T., Takahashi, K., Kanae, S., 2013b. A global water scarcity assessment under shared socio-economic pathways – part 2: water availability and scarcity. Hydrol. Earth Syst. Sci. 17 (7), 2393–2413. https://doi.org/10.5194/hess-17-2393-2013.
Hanasaki, N., Yoshikawa, S., Kakinuma, K., Kanae, S., 2016. A seawater desalination scheme for global hydrological models. Hydrol. Earth Syst. Sci. 20 (10), 1–25.
Hanasaki, N., Yoshikawa, S., Pokhrel, Y., Kanae, S., 2018. A global hydrological simulation to specify the sources of water used by humans. Hydrol. Earth Syst. Sci. 22 (1), 789–817.
Hejazi, M.I., Edmonds, J., Clarke, L., Kyle, P., Davies, E., Chaturvedi, V., Wise, M., Patel, P., Eom, J., Calvin, K., 2014. Integrated assessment of global water scarcity over the 21st century under multiple climate change mitigation policies. Hydrol. Earth Syst. Sci. 18 (8), 2859–2883.
Hejazi, M.I., Voisin, N., Liu, L., Bramer, L.M., Fortin, D.C., Hathaway, J.E., Huang, M., Kyle, P., Leung, L.R., Li, H.-Y., 2015. 21st century United States emissions mitigation could increase water stress more than the climate change it is mitigating. Proc. Natl. Acad. Sci. 112 (34), 10635–10640.
Hempel, S., Frieler, K., Warszawski, L., Schewe, J., Piontek, F., 2013. A trend-preserving bias correction–the ISI-MIP approach. Earth System Dynamics 4 (2), 219–236.
Huang, Z., Hejazi, M., Li, X., Tang, Q., Leng, G., Liu, Y., Döll, P., Eisner, S., Gerten, D., Hanasaki, N., Wada, Y., 2018. Reconstruction of global gridded monthly sectoral water withdrawals for 1971–2010 and analysis of their spatiotemporal patterns. Hydrol. Earth Syst. Sci. 22 (4), 2117–2133. https://doi.org/10.5194/hess-22-2117-2018.
Huang, Z., Hejazi, M., Tang, Q., Vernon, C.R., Liu, Y., Chen, M., Calvin, K., 2019a. Global agricultural green and blue water consumption under future climate and land use changes. J. Hydrol. 574, 242–256.
Huang, Z., Tang, Q., Lo, M.-H., Liu, X., Lu, H., Zhang, X., Leng, G., 2019b. The influence of groundwater representation on hydrological simulation and its assessment using satellite-based water storage variation. Hydrol. Process. 33 (8), 1218–1230. https://doi.org/10.1002/hyp.13393.
Jiang, Y., 2009. China's water scarcity. J. Environ. Manag. 90 (11), 3185–3196.
Jones, B., O'Neill, B.C., 2016. Spatially explicit global population scenarios consistent with the shared socioeconomic pathways. Environ. Res. Lett. 11 (8), 084003.
Joseph, N., Ryu, D., Malano, H.M., George, B., Sudheer, K.P., 2020. A review of the assessment of sustainable water use at continental-to-global scale. Sustainable Water Resources Management 6 (2), 1–20.
Kim, S.H., Edmonds, J., Lurz, J., Smith, S.J., Wise, M., 2006. The ObjECTS framework for integrated assessment: hybrid modeling of transportation. Energy J. 63–91.
Kim, S.H., Hejazi, M., Liu, L., et al., 2016. Balancing global water availability and use at basin scale in an integrated assessment model. Clim. Change 136 (2), 217–231. https://doi.org/10.1007/s10584-016-1604-6.
Kliot, N., 2005. Water Resources and Conflict in the Middle East. Routledge.
Le Page, Y., West, T.O., Link, R., Patel, P., 2016. Downscaling land use and land cover from the global change assessment model for coupling with earth system models. Geosci. Model Dev. 9 (9), 3055–3069. https://doi.org/10.5194/gmd-9-3055-2016.
Liang, X., Lettenmaier, D.P., Wood, E.F., Burges, S.J., 1994. A simple hydrologically based model of land surface water and energy fluxes for general circulation models. Journal of Geophysical Research: Atmospheres 99 (D7), 14415–14428.
Liu, J., Liu, Q., Yang, H., 2016. Assessing water scarcity by simultaneously considering environmental flow requirements, water quantity, and water quality. Ecol. Indic. 60, 434–441.
Liu, X., Tang, Q., Liu, W., Veldkamp, T.I. E., Boulange, J., Liu, J., et al. (2019), A spatially explicit assessment of growing water stress in China from the past to the future. Earth's Future,7(9), 1027–1043. doi:https://doi.org/10.1029/2019EF001181.
Liu, J., Yang, H., Gosling, S.N., Kummu, M., Flörke, M., Pfister, S., et al., 2017. Water scarcity assessments in the past, present, and future. Earth's Future 5 (6), 545–559.
Ma, T., Sun, S., Fu, G., Hall, J.W., Ni, Y., He, L., Cheng, W., 2020. Pollution exacerbates China's water scarcity and its regional inequality. Nat. Commun. 11.
Mekonnen, M.M., Hoekstra, A.Y., 2016. Four billion people facing severe water scarcity. Sci. Adv. 2 (2), e1500323.

Molle, F., Berkoff, J., 2009. Cities vs. agriculture—a review of intersectoral water re-allocation. Nat. Res. Forum 33, 6–18.

Munia, H., Guillaume, J.H.A., Mirumachi, N., Porkka, M., Wada, Y., Kummu, M., 2016. Water stress in global transboundary river basins: significance of upstream water use on downstream stress. Environ. Res. Lett. 11 (1), 014002.

Munia, H.A., Guillaume, J.H.A., Mirumachi, N., Wada, Y., Kummu, M., 2018. How down-stream sub-basins depend on upstream inflows to avoid scarcity: typology and global analysis of transboundary rivers. Hydrol. Earth Syst. Sci. 22, 2795–2809.

Munia, H. A., Guillaume, J. H., Wada, Y., Veldkamp, T., Virkki, V., & Kummu, M. (2020). Future transboundary water stress and its drivers under climate change: a global study. Earth's Future, 8(7), e2019EF001321.

Oki, T., Kanae, S., 2006. Global hydrological cycles and world water resources. Science 313 (5790), 1068–1072.

O'Neill, B.C., Kriegler, E., Riahi, K., Ebi, K.L., Hallegatte, S., Carter, T.R., Mathur, R., van Vuuren, D.P., 2014. A new scenario framework for climate change research: the con-cept of shared socioeconomic pathways. Clim. Chang. 122 (3), 387–400.

Pastor, A.V., Ludwig, F., Biemans, H., Hoff, H., Kabat, P., 2014. Accounting for environmen-tal flow requirements in global water assessments. Hydrol. Earth Syst. Sci. 18 (12), 5041–5059. https://doi.org/10.5194/hess-18-5041-2014.

Pastor, A.V., Palazzo, A., Havlik, P., Biemans, H., Wada, Y., Obersteiner, M., Ludwig, F., 2019. The global nexus of food–trade–water sustaining environmental flows by 2050. Na-ture Sustainability 2 (6), 499–507.

Piani, C., Weedon, G.P., Best, M., Gomes, S.M., Viterbo, P., Hagemann, S., Haerter, J.O., 2010. Statistical bias correction of global simulated daily precipitation and temperature for the application of hydrological models. J. Hydrol. 395 (3), 199–215.

Pires, A., Morato, J., Peixoto, H., Botero, V., Zuluaga, L., Figueroa, A., 2017. Sustainability as-sessment of indicators for integrated water resources management. Sci. Total Envi-ron. 578, 139–147.

Portmann, F.T., Döll, P., Eisner, S., Flörke, M., 2013. Impact of climate change on renewable groundwater resources: assessing the benefits of avoided greenhouse gas emissions using selected CMIP5 climate projections. Environ. Res. Lett. 8 (2), 024023.

Rockström, J., Steffen, W., Noone, K., Persson, Å., Chapin III, F.S., Lambin, E.F., Lenton, T.M., Scheffer, M., Folke, C., Schellnhuber, H.J., 2009. A safe operating space for humanity. Nature 461 (7263), 472.

Rosegrant, M.W., Meijer, S., Cline, S.A., 2012. International model for policy analysis of ag-ricultural commodities and trade (IMPACT): model description. Int. food policy res. Inst. Wash. DC, 28.

Samir, K., Wolfgang, L., 2017. The human core of the shared socioeconomic pathways: population scenarios by age, sex and level of education for all countries to 2100. Glob. Environ. Chang. 42, 181–192. https://doi.org/10.1016/j.gloenvcha.2014.06.004.

Schewe, J., Heinke, J., Gerten, D., Haddeland, I., Arnell, N.W., Clark, D.B., et al., 2014. Multimodel assessment of water scarcity under climate change. Proc. Natl. Acad. Sci. 111 (9), 3245–3250.

Stacke, T., Hagemann, S., 2012. Development and evaluation of a global dynamical wet-lands extent scheme. Hydrol. Earth Syst. Sci. 16 (8), 2915–2933. https://doi.org/10.5194/hess-16-2915-2012.

Sun, S., Fu, G., Bao, C., Fang, C., 2019. Identifying hydro-climatic and socioeconomic forces of water scarcity through structural decomposition analysis: a case study of Beijing city. Sci. Total Environ. 687, 590–600.

Tang, Q., 2020. Global change hydrology: terrestrial water cycle and global change. Sci. China Earth Sci. 63, 459–462. https://doi.org/10.1007/s11430-019-9559-9.

Tang, Q., Lettenmaier, D.P., 2012. 21st century runoff sensitivities of major global river ba-sins. Geophys. Res. Lett. 39 (6).

Tang Q & Oki T. (2016). Terrestrial water cycle and climate change: Natural and human-induced impacts, American Geophysical Union (AGU) Geophysical Monograph Se-ries, Vol 221. Hoboken: John Wiley & Sons. 252pp.

Turner, S.W.D., Hejazi, M., Yonkofski, C., Kim, S.H., Kyle, P., 2019. Influence of groundwater extraction costs and resource depletion limits on simulated global nonrenewable water withdrawals over the twenty-first century. Earth's Future 7, 123–135. https://doi.org/10.1029/2018EF001105.

UN, 2018. Goal 6: ensure access to water and sanitation for all. https://www.un.org/sustainabledevelopment/water-and-sanitation/.

Van Vliet, M.T., Jones, E.R., Flörke, M., Franssen, W.H., Hanasaki, N., Wada, Y., Yearsley, J.R., 2021. Global water scarcity including surface water quality and expansions of clean water technologies. Environ. Res. Lett. 16 (2), 024020.

Vanham, D., Hoekstra, A.Y., Wada, Y., Bouraoui, F., De Roo, A., Mekonnen, M.M., et al., 2018. Physical water scarcity metrics for monitoring progress towards SDG target 6.4: an evaluation of indicator 6.4. 2 "level of water stress". Sci. Total Environ. 613, 218–232.

Veldkamp, T.I.E., Wada, Y., Aerts, J.C.J.H., Döll, P., Gosling, S.N., Liu, J., Masaki, Y., Oki, T., Ostberg, S., Pokhrel, Y., Satoh, Y., Kim, H., Ward, P.J., 2017. Water scarcity hotspots travel downstream due to human interventions in the 20th and 21st century. Nat. Commun. 8, 15697. https://doi.org/10.1038/ncomms15697.

Vernon, C.R., Le Page, Y., Chen, M., Huang, M., Calvin, K.V., Kraucunas, I.P., Braun, C.J., 2018. Demeter–a land use and land cover change disaggregation model. Journal of Open Research Software 6 (1).

Vörösmarty, C.J., Green, P., Salisbury, J., Lammers, R.B., 2000. Global water resources: vul-nerability from climate change and population growth. Science 289 (5477), 284–288.

Vörösmarty, C.J., Douglas, E.M., Green, P.A., Revenga, C., 2005. Geospatial indicators of emerging water stress: an application to Africa. AMBIO: A journal of the Human En-vironment 34 (3), 230–237.

Vörösmarty, C.J., McIntyre, P.B., Gessner, M.O., Dudgeon, D., Prusevich, A., Green, P., Glidden, S., Bunn, S.E., Sullivan, C.A., Liermann, C.R., Davies, P.M., 2010. Global threats to human water security and river biodiversity. Nature 467, 555. https://doi.org/10.1038/nature09440.

van Vuuren, D. P., Kriegler, E., O'Neill, B. C., Ebi, K. L., Riahi, K., Carter, T. R., Edmonds, J., Hallegatte, S., Kram, T., and Mathur, R. (2014), A new scenario framework for climate change research: scenario matrix architecture. Clim. Chang., 122(3), 373–386.

Wada, Y., Beek, L.P.H.V., Viviroli, D., Dürr, H.H., Weingartner, R., Bierkens, M.F.P., 2011. Global monthly water stress: 2. Water demand and severity of water stress. Water Resour. Res. 47 (7), 197–203.

Wada, Y., Wisser, D., Bierkens, M.F., 2014. Global modeling of withdrawal, allocation and consumptive use of surface water and groundwater resources. Earth System Dynam-ics 5 (1), 15–40.

Wada, Y., Flörke, M., Hanasaki, N., Eisner, S., Fischer, G., Tramberend, S., Satoh, Y., Van Vliet, M., Yillia, P., Ringler, C., 2016. Modeling global water use for the 21st century: Water Futures and Solutions (WFaS) initiative and its approaches. Geosci. Model Dev. 9, 175–222.

Wang, Y., Yang, J., Chang, J., 2019. Development of a coupled quantity-quality-environment water allocation model applying the optimization-simulation method. J. Clean. Prod. 213, 944–955.

Warszawski, L., Frieler, K., Huber, V., Piontek, F., Serdeczny, O., et al., 2014. The Inter-Sectoral Impact Model Intercomparison Project (ISI-MIP): project framework. Proc. Natl. Acad. Sci. 111, 3228–3232. https://doi.org/10.1073/pnas.1312330110.

West, T.O., Le Page, Y., Huang, M., Wolf, J., Thomson, A.M., 2014. Downscaling global land cover projections from an integrated assessment model for use in regional analyses: results and evaluation for the US from 2005 to 2095. Environ. Res. Lett. 9 (6), 064004.

Wisser, D., Frolking, S., Douglas, E.M., Fekete, B.M., Schumann, A.H., Vörösmarty, C.J., Hoff, H., Falkenmark, M., Gerten, D., Gordon, L., 2010. The significance of local water re-sources captured in small reservoirs for crop production - a global-scale analysis. J. Hydrol. 384 (3), 264–275.

Yan, D., Yao, M., Ludwig, F., Kabat, P., Huang, H.Q., Hutjes, R.W., Werners, S.E., 2018. Ex-ploring future water shortage for large river basins under different water allocation strategies. Water Resour. Manag. 32 (9), 3071–3086.

Yin, Y., Tang, Q., Liu, X., Zhang, X., 2017. Water scarcity under various socio-economic pathways and its potential effects on food production in the Yellow River basin. Hydrol. Earth Syst. Sci. 21 (2), 791–804.

Yin, Y., Wang, L., Wang, Z., Tang, Q., Piao, S., & Chen, D., et al. (2020). Quantifying water scarcity in northern China within the context of climatic and societal changes and south-to-north water diversion. Earth's Future, 8, e2020EF001492. doi:https://doi.org/10.1029/2020EF001492.

Yin, J., Guo, S., Gentine, P., Sullivan, S. C., Gu, L., He, S., ... & Liu, P. (2021). Does the hook structure constrain future flood intensification under anthropogenic climate warming?. Water Resour. Res., e2020WR028491.

YRCC (Yellow River Conservancy Commission), 2013. Comprehensive Planning of Yellow River Basin (2012—2030). The Yellow River Water Conservancy Press, Zhengzhou, China (in Chinese.

Zawahri, N.A., 2009. India, Pakistan and cooperation along the Indus River system. Water Policy 11 (1), 1–20.

Zhang, X., Tang, Q., Liu, X., Leng, G., Di, C., 2018. Nonlinearity of runoff response to global mean temperature change over major global river basins. Geophys. Res. Lett. 45 (12), 6109–6116.

Zhao, X., Liu, J., Liu, Q., Tillotson, M.R., Guan, D., Hubacek, K., 2015. Physical and virtual water transfers for regional water stress alleviation in China. Proc. Natl. Acad. Sci. 112 (4), 1031–1035.

Zhou, F., Bo, Y., Ciais, P., Dumas, P., Tang, Q., Wang, X., et al., 2020. Deceleration of China's human water use and its key drivers. Proc. Natl. Acad. Sci. 117 (14), 7702. https://doi.org/10.1073/pnas.1909902117.

Zhou, Y., Xu, Y.J., Xiao, W., Wang, J., Huang, Y., Yang, H., 2017. Climate change impacts on flow and suspended sediment yield in headwaters of high-latitude regions—a case study in China's far northeast. Water. 9 (12), 966. https://doi.org/10.3390/w9120966.